



Understanding the behavior of phenylurazole-tyrosine-click electrochemical reaction using hybrid electroanalytical techniques

Ranil C T Temgoua, Fabiola T Dontsi, Estelle Lebègue, Christine Thobie-Gautier, Ignas K Tonlé, Mohammed Boujtita

► To cite this version:

Ranil C T Temgoua, Fabiola T Dontsi, Estelle Lebègue, Christine Thobie-Gautier, Ignas K Tonlé, et al.. Understanding the behavior of phenylurazole-tyrosine-click electrochemical reaction using hybrid electroanalytical techniques. *Journal of Pharmaceutical and Biomedical Analysis*, 2024, 245, pp.116147. <10.1016/j.jpba.2024.116147>. <hal-04824132>

HAL Id: hal-04824132

<https://hal.science/hal-04824132v1>

Submitted on 6 Dec 2024

HAL is a multi-disciplinary open access archive for the deposit and dissemination of scientific research documents, whether they are published or not. The documents may come from teaching and research institutions in France or abroad, or from public or private research centers.

L'archive ouverte pluridisciplinaire **HAL**, est destinée au dépôt et à la diffusion de documents scientifiques de niveau recherche, publiés ou non, émanant des établissements d'enseignement et de recherche français ou étrangers, des laboratoires publics ou privés.



Distributed under a Creative Commons CC BY 4.0 - Attribution - International License



Understanding the behavior of phenylurazole-tyrosine-click electrochemical reaction using hybrid electroanalytical techniques

Ranil C.T. Temgoua^{a,b,*}, Fabiola T. Dontsi^b, Estelle Lebègue^a, Christine Thobie-Gautier^a, Ignas K. Tonlé^b, Mohammed Boujtita^a

^a Nantes Université, CNRS, CEISAM UMR 6230, Nantes F-44000, France

^b University of Dschang, Electrochemistry and Chemistry of Materials, Department of Chemistry, Dschang, Cameroon

ARTICLE INFO

Keywords:

Bioconjugation
Chemo-selectivity
Click reactions
Cyclic voltammetry
Coulometry
Mass spectrometry

ABSTRACT

In this work, the electrochemical behavior of 4-phenylurazole (Ph-Ur) was studied and the latter was used as a molecular anchor for the electrochemical bioconjugation of tyrosine (Y). Cyclic voltammetry (CV) and controlled potential coulometry (CPC) allowed the *in-situ* generation of the PTAD (4-phenyl-3 H-1,2,4-triazole-3,5(4 H)-dione) species from phenylurazole on demand for tyrosine electrolabeling. The chemoselectivity of the reaction was studied with another amino acid (lysine, Lys) and no changes in Lys were observed. To evaluate the performance of tyrosine electrolabeling, coulometric analyses at controlled potentials were performed on solutions of phenylurazole and the phenylurazole-tyrosine mixture in different proportions (2:1, 1:1, and 1:2). The electrolysis of the phenylurazole-tyrosine mixture in the ratio (1:2) produced a charge of 2.07 C, very close to the theoretical value (1.93 C), with high reaction kinetics, a result obtained here for the first time. The products obtained were identified and characterized by liquid chromatography coupled to high-resolution electrospray ionization mass spectrometry (LC-HRMS and LC-HRMS²). Two products were formed from the click reactions, one of which was the majority. Another part of this work was to study the electrochemical degradation of the molecular anchor 4-phenylurazole (Ph-Ur). Four stable degradation products of phenylurazole were identified (C₇H₉N₂O, C₆H₈N, C₆H₈NO, C₁₄H₁₃N₄O₂) based on chromatographic profiles and mass spectrometry results. The charge generated during the electrolysis of phenylurazole (two-electron process) (2.85 C) is inconsistent with the theoretical or calculated charge (1.93 C), indicating that secondary/parasitic reactions occurred during the electrolysis of the latter. In conclusion, the electrochemically promoted click phenylurazole-tyrosine reactions give rise to click products with high reaction kinetics and yields in the (1:2) phenylurazole-tyrosine ratios, and the presence of side reactions is likely to affect the yield of the click phenylurazole-tyrosine reaction.

1. Introduction

The development of a site-selective, gentle and biocompatible reaction for the modification of biomolecules is a breakthrough in chemical biology, medicine and clinical pharmacology. By attaching synthetic molecules to a specific position on proteins, a new concept is emerging: bioconjugation. Bioconjugation is a tool at the interface of biology and chemistry that involves the formation of covalent bonds between a biomolecule and any other molecule. [1]. Thus, several so-called bio-orthogonal bioconjugation/ligation methods have been widely explored for the development of protein conjugates. These are of considerable

importance in various fields, such as the conjugation of toxins, imaging agents or radiopharmaceuticals to monoclonal antibodies in cancer therapy, the design of glycoconjugate vaccines, the modification of antibody drugs, and the development of drug delivery systems [2].

Direct modification of proteins is generally performed at the amino lysine group with N-hydroxysuccinimide-activated esters or sulfonyl chlorides. Alternatively, cysteine residues can be modified by disulfide exchange and Michael addition for single site functionalization [3]. In comparison, the remaining eighteen amino acids have been much less explored [4]. Recently, click reactions specifically targeting tyrosine residues have emerged as a promising alternative. Electrochemically

* Corresponding author at: Nantes Université, CNRS, CEISAM UMR 6230, Nantes F-44000, France.

E-mail address: raniltemgoua@yahoo.fr (R.C.T. Temgoua).

¹ Ranil C. T. Temgoua is currently working in the Department of Analytical Chemistry and Reference Materials, Bundesanstalt für Materialforschung und-prüfung (BAM), Berlin, Germany.

<https://doi.org/10.1016/j.jpba.2024.116147>

Received 9 December 2023; Received in revised form 9 April 2024; Accepted 10 April 2024

Available online 18 April 2024

0731-7085/© 2024 The Author(s). Published by Elsevier B.V. This is an open access article under the CC BY license (<http://creativecommons.org/licenses/by/4.0/>).

initiated modification of tyrosine residues has been enabled by urazole anchors, which are drug-based compounds that act as antifungal and anti-inflammatory agents [5]. The electrochemical oxidation product of phenylurazole (4-phenyl-3 H-1,2,4-triazole-3,5(H)-dione; PTAD) reacts with the phenolic side chain of tyrosine via an ene-type reaction [6]. The method proved to be relatively chemoselective for tyrosine, allowing specific modification of peptides and proteins.

Tyrosine residues represent an attractive target for the labeling of biomolecules due to their low natural abundance on the protein surface. Several methods for tyrosine modification have been developed, including enzymatic and chemical methods (Mannich-type reactions, metal-catalyzed oxidations, rhodium salts, single electron transfer catalysts) [7]. The use of molecular anchors such as N-methyluminol and phenylurazole derivatives is second to none in this modification and has been extensively exploited by the Barbas group [8]. Alvarez-Dorta and co-authors [9] have developed another electrochemical method for protein bioconjugation (e-Y-click). The e-Y-click (electrochemical-tyrosine click) reaction was applied under optimized conditions to label angiotensin II, which is a hormone that regulates blood pressure. Phenylurazole was used as the molecular anchor, the conjugate was obtained with a conversion rate of 83 % and no protein degradation was observed during the reaction according to HPLC and MS profiles. A similar work was developed by Depienne and co-authors. In the course of their work, phenylurazole (Ph-Ur), N-methylphenylurazole (NMePhUr) and N-methyluminol (NMeLum) derivatives were described as tyrosine (Y) anchors after chemical or enzymatic oxidation. The results demonstrated a high efficiency of NMeLum, which showed complete Y-chemoselectivity on polypeptides and biologically relevant proteins after gentle electrochemical activation [10].

Despite all these works, no studies have been reported to elucidate the Y-chemoselectivity character of phenylurazole-tyrosine e-click reaction. This work aims to demonstrate that the electrochemical oxidation of phenylurazole in the "on demand" mode in the presence of tyrosine is the key of the obtained Y-chemoselectivity of the labeling reaction. Therefore, electrochemical methods were used to generate the oxidation products. An appropriate electrochemical potential was applied to activate the resting Ph-Ur species *in situ*, on demand, without oxidizing the sensitive amino acids of the protein or the ligands attached to the Ph-Ur. The Ph-Ur degradation products and the formation products of the phenylurazole-tyrosine click reaction were characterized by LC-HRMS and tandem LC-HRMS².

2. Material and method

2.1. Reagents

Ammonium acetate (NH₄OAc), formic acid (HCOOH), Ph-Ur, Y and Lys were purchased from Sigma-Aldrich (St. Quentin-Fallavier, France). Methanol (MeOH) and acetonitrile (CH₃CN) (both in gradient grade quality for UPLC-MS) were purchased from Sigma-Aldrich. All other commercially available chemicals and reagents were of the highest quality available. Ultrapure water was used in all the experiments.

2.2. Electrochemical conditions (EC): Cyclic voltammetry (CV), controlled potential electrolysis (CPE) and mass voltammetry (EC-MS)

The electrochemical behavior of Ph-Ur, Y and Lys was investigated in the presence of ammonium acetate (ESI-MS friendly electrolyte). Ammonium acetate was dissolved to a concentration of 100 mM in H₂O/MeCN (50/50, v/v) solution, pH 7.4. CV measurements were performed using a VSP potentiostat controlled by EC-Lab V10.40 software from Bio-Logic Science Instruments (Seyssinet-Pariset, France). A three-electrode system consisting of a glassy carbon working electrode (GCE, 2.0 mm diameter, geometric surface area of 0.031 cm²), a metallic stainless steel counter electrode and a saturated calomel reference electrode (SCE) was used. Knowledge of the $I = f(E)$ curve at a given electrode, which is

related to the redox behavior of Ph-Ur, made it possible to determine its electrolysis potential.

CPE was performed on a VSP potentiostat with a three-electrode system consisting of a graphite crucible working electrode (surface area: 9.5 cm²), a saturated calomel reference electrode (SCE), and a metallic (stainless steel) auxiliary electrode placed in a separate cathode compartment. Electrolysis was performed in a 0.1 M ammonium acetate solution (pH 7.4) in H₂O/MeCN (50/50, v/v) at a given potential. 1 mM Ph-Ur was electrolyzed in a stirred solution in a total volume of 10 mL for 4 h in the absence and in the presence of various proportions of Y. Samples were collected in vials and stored at - 18 °C until analysis.

For mass voltammetry experiments (measurement of m/z intensity as a function of the potential applied to the working electrode) experiments, an EmStat potentiostat controlled by PSTrace software from PalmSens Instruments was equipped with a commercially available electrochemical thin-layer μ PrepCell™ (Antec Scientific, Zoeterwoude, The Netherlands) and a syringe pump (gas-tight syringe 549–0538, VWR Collection, Rosny-sous-Bois, France). A three-electrode configuration was used in the present study, i.e., a boron-doped diamond (BDD) working electrode ($A = 1.9 \text{ cm}^2$), a HyREF™ palladium-hydrogen (Pd/H₂) reference electrode, and the carbon-loaded PTFE (polytetrafluoroethylene) auxiliary electrode. The EC cell outlet was connected directly to the electrospray source inlet of a Xevo G2-XS QT of the mass spectrometer. Typically, 0.1 mM of Ph-Ur and Ph-Ur+Y solutions in a 20 mM ammonium acetate solution (pH 7.4) in H₂O/MeCN (50/50, v/v) were pumped through the electrochemical cell at a flow rate of 25 $\mu\text{L}/\text{min}$. The cell potential was ramped from 0 V to 1 V versus a Pd/H₂ pseudo reference electrode at the rate of 10 mV/s. Representative results from at least three independent experiments were considered. When necessary, the BDD working electrode was activated (potential E1, +2 V; potential E2, -2 V; potential E3, 0 V; time t1, 1000 ms; time t2, 1000 ms; time t3, 0 ms; continuously changing for 5 min) with a 0.5 M of nitric acid solution as described by the manufacturer (Antec Scientific). The experiment was carried out in triplicate.

2.3. LC-MS conditions: Liquid chromatography coupled to mass spectrometry

Analyses were performed on an Acquity UPLC H-Class system (Waters, Guyancourt, France) coupled to a quadrupole time-of-flight (QToF) mass spectrometer through an electrospray ionization (ESI) interface in the positive ionization mode (Xevo G2-XS QToF, Waters, Guyancourt, France). Analysis and data processing were performed using MassLynx software, version 4.1.

The separation was performed at 25 °C on an Acquity UPLC BEH-C18 column (130 Å, 1.7 μm , 2.1 mm \times 50 mm). Samples were eluted from the LC column using the following linear gradient (curve number 6): 0–0.4 min, 5 % B; 0.4–4 min, 5–60 % B; 4–5 min, 60 % B; 5–6 min, 60–100 % B; 6–6.5 min, 100–5 % B; 6.5–8 min, 5 % B. Solvent A was H₂O and solvent B was MeCN, both solvents containing 0.1 % HCOOH. The injection volume was set to 2 μL and the chromatographic flow rate was set to 0.4 mL.min⁻¹.

A Q-TOF mass spectrometer equipped with an ESI interface was operated in negative and positive ion mode for detection of m/z in the range of 50–1200 at 2 Hz. Capillary voltage, cone voltage, desolvation gas flow (N₂), cone gas flow (N₂), source temperature, and desolvation temperature were set to 0.5 kV, 80 V, 80 L.hr-1, 600 L/h, 120 °C, and 350 °C, respectively. MSMS experiments were performed with a collision energy ramp from 10 to 40 V in the presence of argon gas. The TOF analyzer was operated in the sensitive mode. The accuracy achieved in the determination of m/z was supported by lock mass. Leucine enkephalin, prepared at 2 $\mu\text{g}/\text{mL}$ in an H₂O/MeCN/HCOOH (50/50/0.1, v/v/v) mixture, was infused into the lock spray channel at a constant flow rate (10 $\mu\text{L}/\text{min}$) (acquired 0.3 s every 15 s). Leucine enkephalin signals at 236.1036 and 554.2615 were used for m/z alignment. Mass traces were extracted for each target molecule with an absolute window

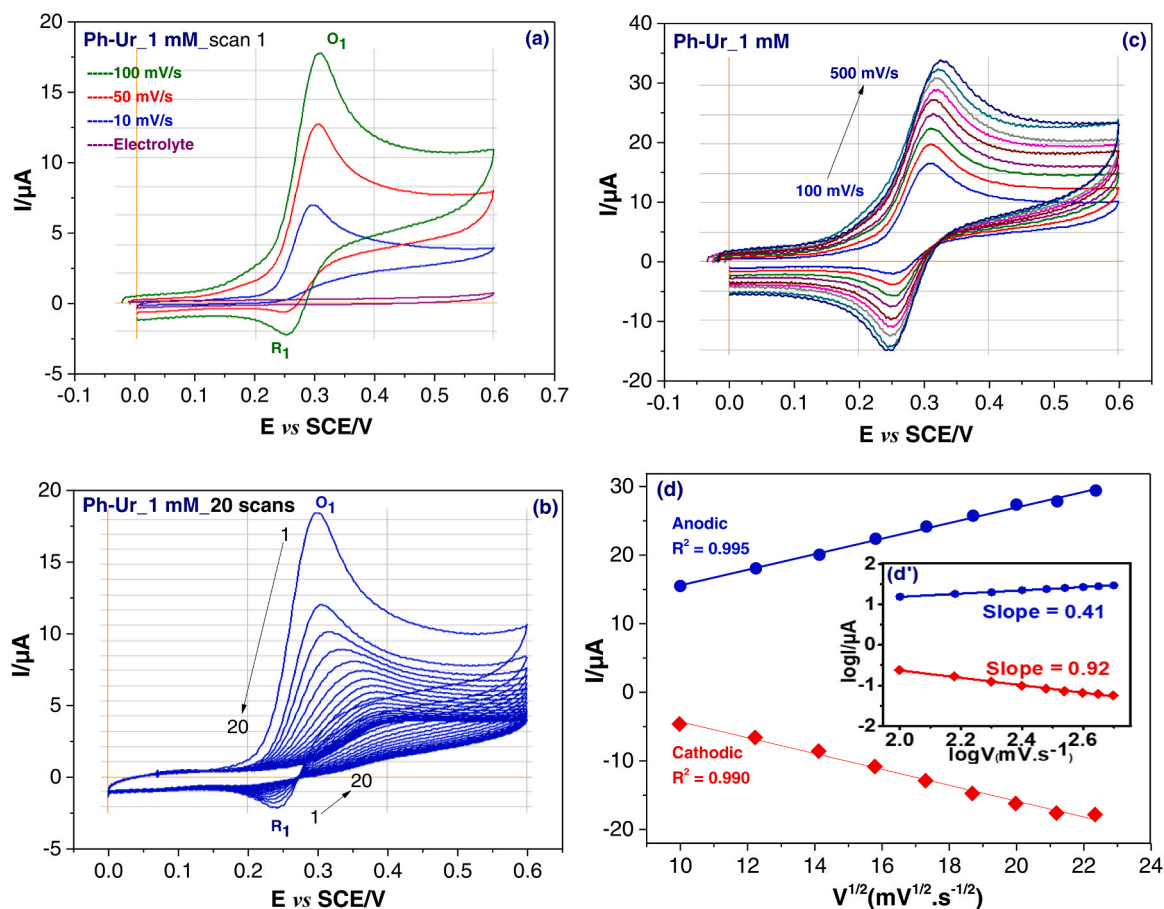
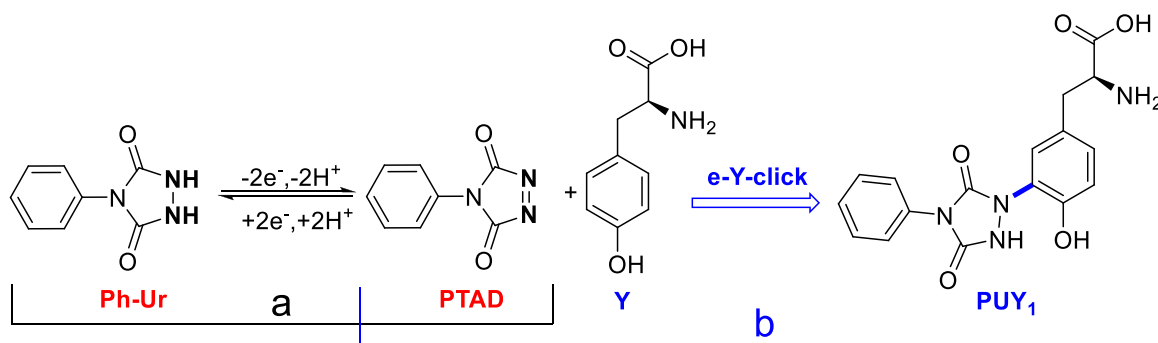


Fig. 1. (a) Cyclic voltammograms of 1.0 mM Ph-Ur recorded on GCE in $\text{H}_2\text{O}/\text{MeCN}$ 50:50 with 0.1 M of NH_4OAc , pH 7.4, scan rate = 10, 50 and 100 mV/s. (b) Multicyclic voltammograms of 1.0 mM Ph-Ur recorded at 100 mV/s. (c) Cyclic voltammograms of 1.0 mM Ph-Ur at different scan rates (100, 150, 200, 250, 300, 350, 400, 450 and 500 mV/s); (d) Peak current as a function of $V^{1/2}$; (d') $\log(I_{pa})$ as a function of $\log(v)$.



Scheme 1. (a) Electrochemical oxidation/activation of 4-phenylurazole and (b) e-Y-click reaction between PTAD and tyrosine (Y).

of 0.01 Da, and data were processed using MassLynx 4.1 software (Waters).

3. Results and discussion

3.1. Electrochemical behavior and study of some kinetic parameters of redox reactions of Ph-Ur

The electrochemical study of Ph-Ur in a 0.1 M ammonium acetate solution (ESI-MS friendly electrolyte) solution (pH 7.4, in $\text{H}_2\text{O}/\text{MeCN}$ 50:50), at GCE was performed using cyclic voltammetry at different scan rates (Fig. 1a,b).

As shown in Fig. 1a, at a low scan rate, the cyclic voltammogram at

10 mV/s shows the characteristic of an irreversible electron transfer process with an anodic peak (O_1) at 0.31 V vs. SCE, corresponding to the conversion of 4-phenylurazole (Ph-Ur) to 4-phenyl-1,2,4-triazole-3,5-dione (PTAD) (Scheme 1) [11]. This behavior is quite different (increase in oxidation current) when the same experiment is performed at a higher scan rate (50, 100 mV/s). In fact, during the reverse scan, a cathodic peak appears at a potential close to 0.25 V vs. SCE with a significantly lower intensity. The amount of compound reduced is proportional to the amount formed during oxidation, and the flow of material to the electrode surface (and therefore the current) is greater as the scan rate increases. In fact, the higher the scan rate, the shorter the time it takes to scan a range of potentials, so at each potential the diffusion layer is weaker and therefore the flow of reagent to the

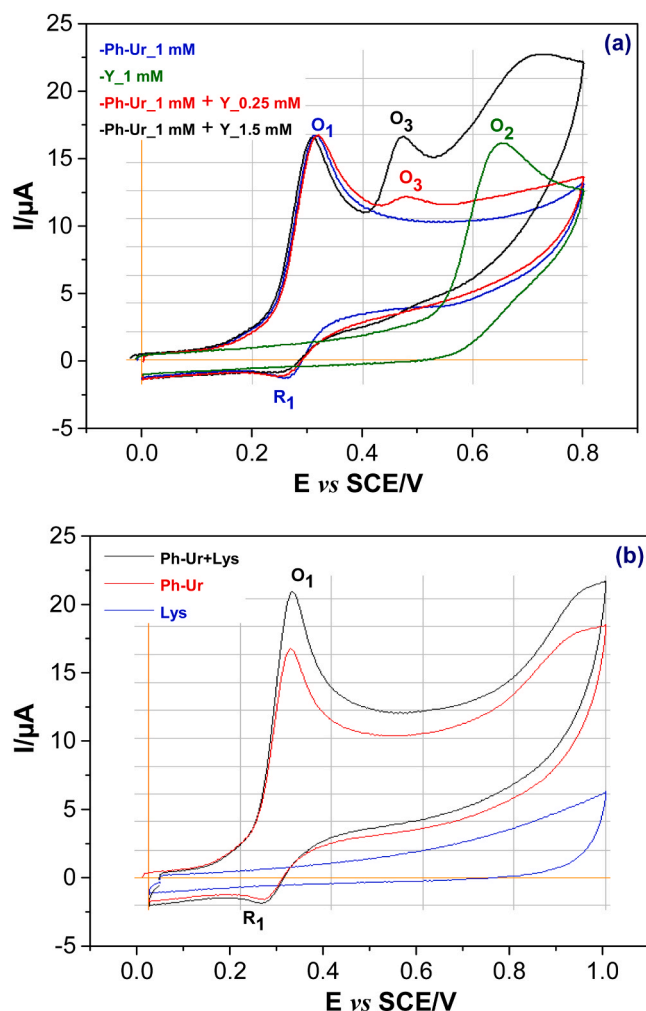


Fig. 2. (a) Cyclic voltammograms of 1.0 mM Ph-Ur in the absence (blue) and in the presence (red and black) of 1.0 mM Y (green) at GCE, in 0.1 M NH₄OAc pH 7.4, scan rate = 100 mV/s. (b) Cyclic voltammograms of 1.0 mM Ph-Ur in the absence (red) and in the presence (black) of 1.0 mM Lys (blue) at GCE, in 0.1 M NH₄OAc pH 7.4, scan rate = 100 mV/s.

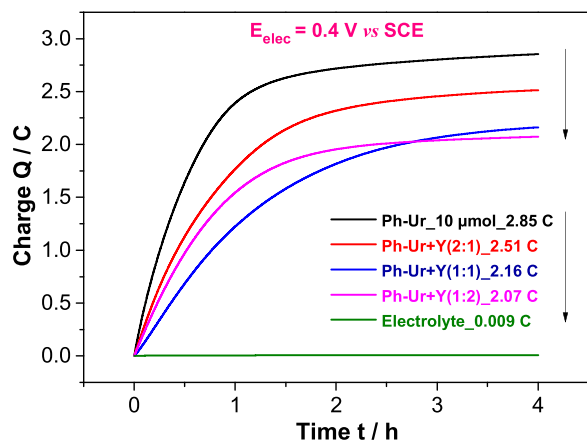


Fig. 3. Charge vs time obtained during the controlled potential electrolysis of Ph-Ur (10 μmol) in the absence and in the presence of various proportion of tyrosine (Y; 5 μmol, 10 μmol and 20 μmol), after 4 h in 0.1 M NH₄OAc pH 7.4. Q_{calc}: theoretical charge; Q_{exp}: experimental charge.

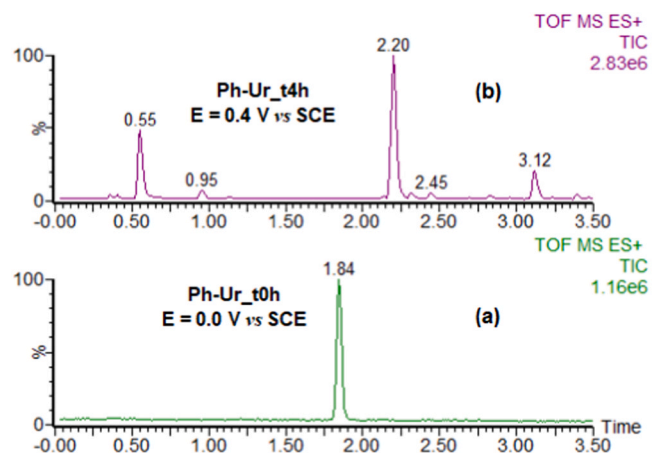


Fig. 4. LC-HRMS chromatograms of Ph-Ur solutions (non-oxidized and electrochemically oxidized) at pH 7.4.

electrode surface is greater. As the reagent flux increases, so does the current density. This behavior can also be explained by the lifetime/-reaction time of the species formed after electrochemical oxidation at the electrode.

In cyclic voltammetry, the potential scan rate is an effective experimental parameter that can be used to control τ , a measure of the time that a stable electroactive species can communicate with the electrode. Increasing the scan rate limits this characteristic time relative to t , where t is the characteristic lifetime of a coupled chemical reaction. In accordance with the work of Varmaghani and co-authors [12] on the behavior and kinetic studies of 4-phenylurazole, an ErCi mechanism was chosen for the electrochemical oxidation of Ph-Ur. For a better understanding of the Ph-Ur behavior at the electrode, multisweep cyclic voltammetry (20 scans) was performed (Fig. 1b). After several scans, a decrease in the anodic and cathodic peak currents (loss of reversibility) can be observed, accompanied by a shift of the anodic peak potentials towards positive values. This behavior could be due to the passivation phenomenon at the electrode, but also to the instability of the product formed after the oxidation of Ph-Ur, which probably remains at the electrode and prevents the further oxidation of the new species, which will diffuse towards the working electrode.

The kinetic parameters were evaluated by studying of the influence of the scan rate. Thus, by varying the potential scan rate (v) between 100 and 500 mV/s, the voltammograms of 1 mM Ph-Ur in a 0.1 M NH₄OAc medium were recorded, and as shown in Fig. 1c, a couple of quasi-reversible redox peaks of Ph-Ur were obtained on each voltammogram at different scan rates. In this variation, the redox peak currents were dependent on the potential scan rate and gradually increased with this parameter. Furthermore, these peak currents show a linear dependence on the square root of the potential scan rate ($v^{1/2}$) (Fig. 1d). This indicates a diffusion-controlled process, which was also confirmed by plotting the double logarithm of I_{pa} vs scan rate (Fig. 1d') with a slope ($\partial \log(I_{pa}) / \partial \log(v)$) equal to 0.41 which is close to the characteristic value (0.5) of a diffusion-controlled electron transfer mechanism [13]. On the other hand, the slope ($\partial \log(I_{pc}) / \partial \log(v)$) for the cathodic part is equal to 0.92. This value is close to the characteristic value (1.0) of an adsorption controlled process. These results therefore show diffusional control for the direct reaction (oxidation) and sorptional control for the reverse process (reduction). This means that the electron transfer product is adsorbed on the electrode and the limiting steps are modified.

3.2. Reactions mechanism of Ph-Ur with tyrosine (Y): e-Y-click

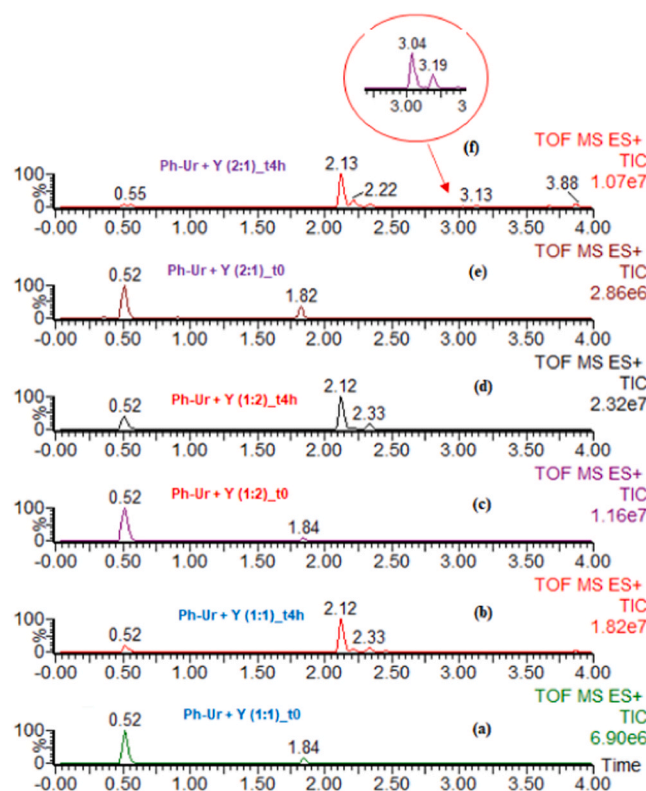
3.2.1. Cyclic voltammetry of Ph-Ur in the presence of Y and lysine (Lys)

In a first assay, the electrochemical oxidation behavior of Ph-Ur was analytically studied, in the presence of L-tyrosine (Y). Cyclic

Table 1

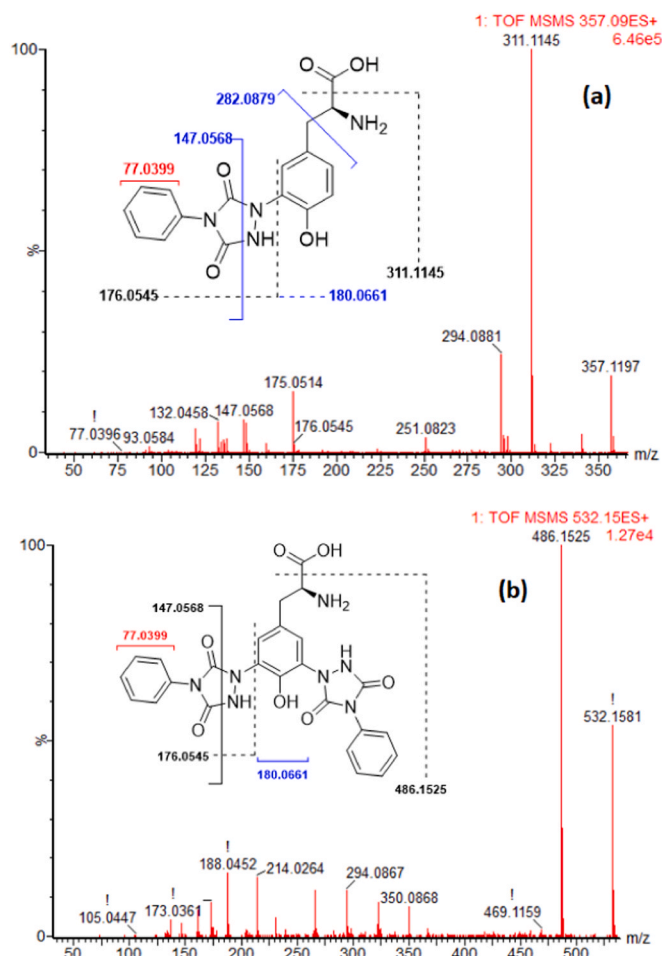
Detected Ph-Ur main oxidation products and clicked products with their exact masses, retention times, mass deviation and molecular formulas.

Compounds	Ions	m/z (exp)	m/z (th)	$\Delta m/z$ (mDa)	$\Delta m/z$ (ppm)	Retention time (min)	Raw formula
Ph-Ur main oxidation products							
Ph-Ur	$[M+H]^+$	178.0626	178.0617	0.9	5.1	1.84	$C_8H_8N_3O_2$
Ph-Ur	$[M-H]^-$	176.0454	176.0460	-0.6	-3.4	1.84	$C_8H_8N_3O_2$
PU ₁	$[M+H]^+$	137.0720	137.0715	0.5	3.6	2.20	$C_7H_9N_2O$
PU ₂	$[M+H]^+$	94.0667	94.0657	1.0	10.6	0.55	C_6H_8N
PU ₃	$[M+H]^+$	110.0583	110.0606	-2.3	-20.9	0.4	C_6H_8NO
PU _{4a,b}	$[M+H]^+$	269.1036	269.1039	-0.3	-1.1	2.45	$C_{14}H_{13}N_4O_2$
		269.1039		0.4	1.5	3.12	
Clicked products Ph-Ur+Y							
Y	$[M+H]^+$	182.0819	182.0817	0.2	1.1	0.52	$C_9H_{12}NO_3$
PUY ₁	$[M+H]^+$	357.1202	357.1199	0.3	0.8	2.12	$C_{17}H_{17}N_4O_5$
PUY ₂	$[M+H]^+$	532.1580	532.1580	-0.1	-0.2	3.04	$C_{25}H_{22}N_7O_7$

PU = Transformation product of Ph-Ur; PUY = Clicked product between Ph-Ur and Y; m/z (th) = theoretical m/z ; m/z (exp) = experimental m/z **Fig. 5.** LC-MS chromatograms of oxidized and non-oxidized solutions of Ph-Ur + Y with various proportions of Y. The solutions were oxidized at 0.4 V at pH 7.4.

voltammograms of the isolated reagent Ph-Ur and Y were recorded (Fig. 2a). The study was performed in a neutral medium (pH 7.4) for physiological relevance.

As shown previously, O_1/R_1 (0.31 V / 0.25 V) represents a quasi-reversible redox system for Ph-Ur. In the case of Y, there is a single oxidation peak O_2 around 0.66 V, indicating an irreversible redox system for this amino acid in this potential range. There is a clear separation between the oxidation peaks of single Ph-Ur and Y. When the same experiment was performed mixing different amounts of Ph-Ur and Y, a new anodic peak O_3 corresponding to the conjugated oxidation product appears at a more positive potential 0.48 V and the cathodic peak R_1 at 0.25 V, corresponding to the PTAD reduction, disappears during the reverse scan, indicating a chemical reaction at the surface of the electrode. The anodic peak O_2 for Y also disappears in the presence of Ph-Ur when the Y is in low concentration. As described by Alvarez-Dorta and co-workers [9], the oxidation of both the phenol

**Fig. 6.** HRMS² spectra of PUY₁ (a) and PUY₂ (b).

moiety present on the Y (O_2) and the clicked product (O_3) appear at an even more positive potential than the Ph-Ur oxidation (O_1), allowing the selective electrochemical activation of the PTAD. It should be noted that the O_1 peak current attributed to Ph-Ur oxidation does not decrease in all situations (with or without Y), proving that the click reaction takes place between tyrosine and the electrochemical oxidation product of Ph-Ur. This clearly shows that there is no chemical reaction between Ph-Ur and Y; any reaction starts after an electrochemical potential is applied to the working electrode. Thus, this analytical study shows that by selecting an appropriate potential of 0.31 V (O_1), the e-Y-Click reaction is achieved without oxidizing the Y reagent or the clicked product. The chemoselectivity of the reaction was investigated using another

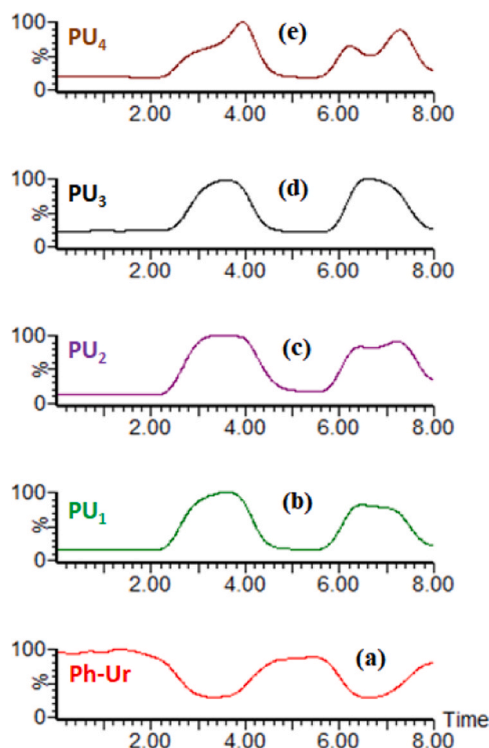


Fig. 7. 2D mass voltammograms of Ph-Ur and its oxidation products PU₁, PU₂, PU₃ and PU₄ using BDD working electrode (scanned 0–1 V vs Pd/H₂ reference electrode, 10 mV/s).

amino acid (L-lysine, Lys). Cyclic voltammograms of Ph-Ur were recorded in the presence of commercially available protected (p) L-lysine (Fig. 2b). L-lysine (electroinactive in the potential range studied) was inert to PTAD and no E_ci mechanisms were detected. The occurrence of a chemical reaction would lead to the appearance of an additional oxidation peak, but also possibly to the disappearance of the cathodic peak R₁, indicating that the PTAD that formed on the surface of the electrode is consumed. There was also a slight increase in the Ph-Ur oxidation peak in the presence of lysine. Currently, we do not fully understand this behavior. However, no Ph-Ur-Lys adduct was observed by HPLC-MS. This result excludes the hypothesis of a catalytic effect of Lys on the Ph-Ur oxidation reaction. Thus, the increase in current observed when L-lysine was added remained insignificant and could be due to a change in the conductivity of the electrolyte solution. Other amino acids (L-phenylalanine, L-tryptophan and L-histidine) were also used to study the chemoselectivity of the e-Y-click reaction, and the results were conclusive [9,10].

3.2.2. Coulometric studies (electrolysis)

The electrolysis conditions were set to produce a unique electrochemical reaction (oxidation in our case) takes place. The controlled potential value (0.4 V vs SCE) suitable for exhaustive electrolysis was selected according to Ph-Ur cyclic voltammograms. A series of electrolysis experiments were then carried out with Ph-Ur and Ph-Ur:Y (different proportions 1:1; 1:2 and 2:1), on a large surface graphite electrode in a 0.1 M of ammonium acetate solution in H₂O/MeCN (50/50, v/v). The electrolysis was stopped when the current decay was close to 90 % (4 h, Fig. 3).

Before discussing Fig. 3, it was important to clarify the theoretical (or calculated) charges generated as a function of electron number for Ph-Ur. Q_{calc} is found to be 0.96 C for a one-electron process, 1.93 C for a two-electron process, 2.89 C for a three-electron process and 3.86 C for a four-electron process. The electrolysis/oxidation of Ph-Ur (a two-electron process) produced a charge of 2.85 C, which is higher than

the expected theoretical charge. This high charge value can be attributed to the oxidation of one or more Ph-Ur degradation products generated during electrolysis. LC-MS analysis can be used to trace these compounds. When Ph-Ur electrolysis is performed in the presence of different proportions of Y, the charges generated depend on the fraction of Y present in the electrochemical reactor. By comparing these charge values, it was found that the charge generated (2.07 C) during the electrolysis of Ph-Ur:Y (1:2) is closer to the theoretical value (1.93 C). For this ratio, the e-Y-click reaction is much more quantitative and the kinetics of the reaction is great, considering the shape of the curve (the curve quickly reaches the plateau). The value of the charge for the ratio Ph-Ur:Y (1:1) is also close to the theoretical value, but the kinetics is slow, given the shape of the curve. This reaction is therefore not sufficiently quantitative for the e-Y-click reaction.

3.2.3. LC-HRMS and LC-HRMS² analysis: Identification and characterization of degradation products of Ph-Ur and formation products of e-Y-click reactions

Experiments were performed in neutral medium (pH 7.4) and electrochemically generated oxidation products of Ph-Ur were identified by LC-HRMS. A unique peak at m/z 178.0617 [M+H]⁺ (ESI+) and m/z 178.0617 [M-H]⁻ (ESI-), R_t = 1.84 min, attributed to Ph-Ur was observed in LC-HRMS when the potential was set at 0 V vs SCE (Fig. 4a). When the potential was set to a value of 0.4 V, the LC-HRMS analysis indicated electrochemical oxidation of Ph-Ur by the observation of new signals (Fig. 4b). It should be noted that the signal of the degradation products was not significant in the negative mode. The positive mode was therefore chosen for subsequent experiments. Therefore, the positive mode was chosen for the following experiments. The study of the electrochemical degradation of Ph-Ur allows, on the one hand, the identification of potential degradation/transformation products of the latter and, on the other hand, a better understanding and control of the e-Y-Click reaction. These degradation products can potentially lead to parasitic reactions during the e-Y-click reaction of interest. LC-HRMS analysis allowed the identification of four stable degradation products. The corresponding molecular weights are summarized in Table 1. The unstable nature of the PTAD does not allow its observation under these conditions.

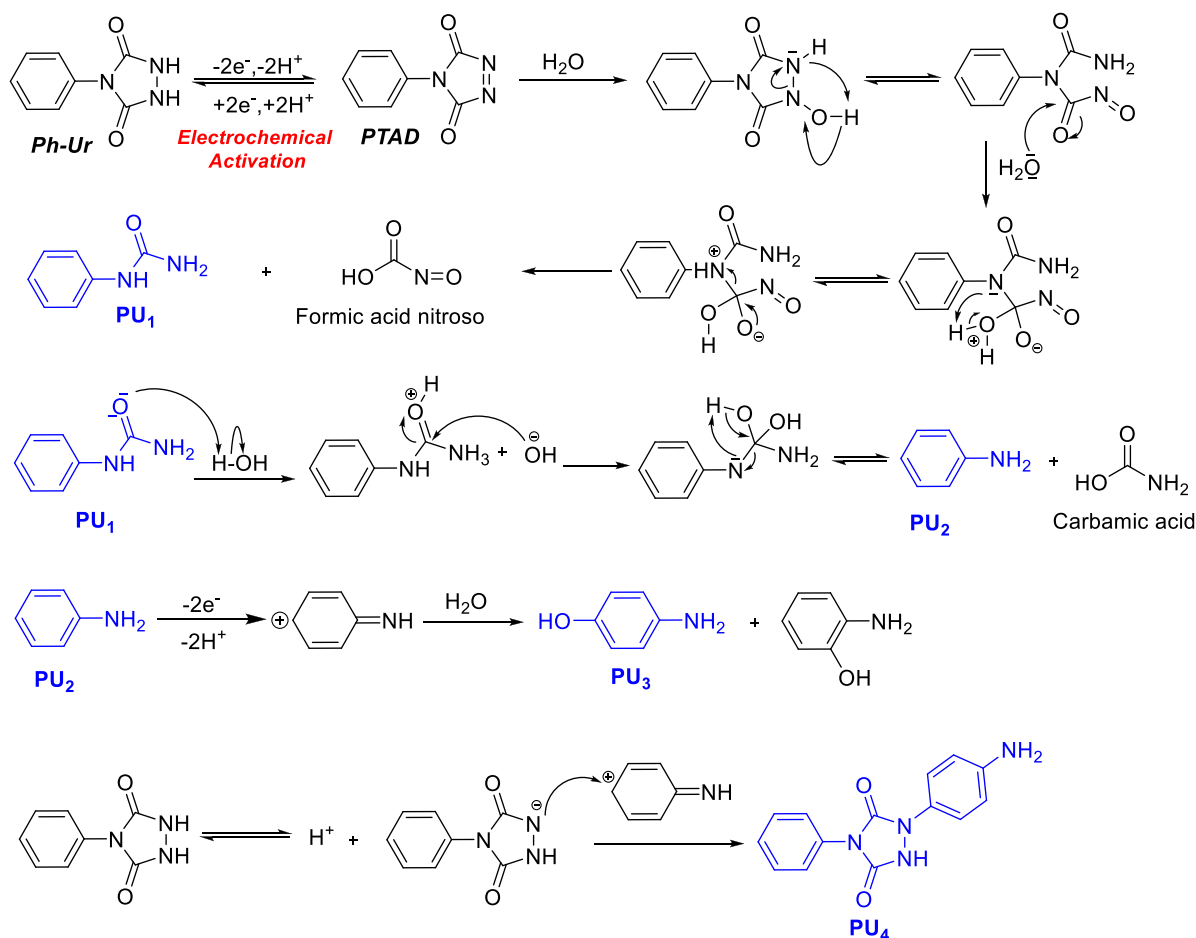
The identification and structural characterization were carried out by obtaining their elemental composition on the mono-isotopic peak (Fig. S11) and confirming their structures by LC-HRMS (Fig. S12) and LC-HRMS² analysis (Fig. S13). Oxidation products named PU₁, PU₂, PU₃ and PU₄ were obtained (Table 1).

The electrolysis of Ph-Ur in the presence of Y resulted mainly in two clicked products, one majority with a retention time of 2.12 min, and the second around 3.04 min which forms very weakly. The elemental composition is given in Table 1 and the chromatograms obtained, before and after electrolysis are shown in Fig. 5. The structures of the two products were confirmed by LC-HRMS² analysis (Fig. 6).

As previously mentioned in Section 3.2.2, the e-Y-click reaction is very quantitative for the ratio Ph-Ur:Y (1:2). The total ionic current intensity, while not an accurate measure of the amount of product formed, is most intense for this ratio.

3.2.4. Online monitoring of degradation of Ph-Ur and e-Y-click reaction

Mass voltammetry was performed to better understand the degradation mechanism of Ph-Ur, but also to follow the e-Y-click reaction in real time. As shown in 7a, the mass voltammogram of the m/z 178.0617 associated to the mono-isotopic peak of Ph-Ur decreases significantly (at about 2.2 min, corresponding to 0.4 V vs Pd/H₂) with the increase of the potential at the working electrode, confirming its oxidation. In the same figure (Fig. 7b,c,d,e), the appearance of the oxidation products PU₁, PU₂, PU₃ and PU₄ was noted in correlation with the decrease of the signal intensity of Ph-Ur, suggesting a correlation between their formation and the electrochemical oxidation of Ph-Ur. The overlay graphs of Fig. 7 are shown in Fig. S14 for additional information. These results irrefutably



Scheme 2. Proposed mechanism of the electrochemical oxidation of Ph-Ur.

confirm that the transformation products originate from the electrochemical oxidation of Ph-Ur and not from any other degradation pathway.

Direct EC-MS and indirect EC-LC-MS techniques allowed during this study to propose an electrochemical oxidation (degradation) mechanism of Ph-Ur. Scheme 2 illustrates this mechanism. These PU_n oxidation products are formed from PTAD, i.e., after a two-electron oxidation process of Ph-Ur. To the best of our knowledge, no study on the electrochemical degradation of Ph-Ur has been reported.

In the presence of tyrosine (Y), the mass voltammogram (Fig. S15) shows, in addition to the oxidation products of Ph-Ur, the appearance of a product for the reaction between PTAD (oxidized form of Ph-Ur) and Y, i.e., the product PUY_1 . These oxidation products, as well as the second reaction product PUY_2 are not highlighted in Fig. S15, because they are masked in the background. Also noteworthy in the same diagram is the decay of the Y signal from a given potential, which indicates that it is consumed during the e-Y-click reaction.

4. Conclusion

The aim of this work was to provide relevant information to elucidate the Y-chemoselectivity of the phenylurazole-tyrosine click reaction by electrochemistry coupled to mass spectrometry for a better understanding of the electrochemical bioconjugation mechanism, which is a promising alternative to peptide and protein conjugation. This work shows that the Ph-Ur-Y reaction is much more quantitative in 1:2 proportions (Ph-Ur:Y) with high reaction kinetics as demonstrated by coulometric analyses. LC-HRMS and LC-HRMS² analyses demonstrated the efficiency of Y labeling with Ph-Ur, with the possibility of double

labeling on Y, but with a very low yield. In addition, four degradation by-products of phenylurazole were identified, which are likely to generate the parasitic/secondary reactions during the phenylurazole-tyrosine click reaction. The future of phenylurazole-tyrosine click reactions in the therapeutic field and in the biotechnology industry is very promising, providing access to the development of many cutting-edge vaccines and drugs, since these reactions are chemo-selective. The use of an electrochemical cell in a flow system could be promising for industrial applications. The use of a flow reactor could provide high electrochemical control for the generation of PTAD species and better control of e-click bioconjugation reactions. However, significant progress needs to be made in limiting mass transport within flow cells, where the flow regime is generally laminar.

CRediT authorship contribution statement

Mohammed Boujtita: Writing – review & editing, Supervision, Project administration, Funding acquisition, Conceptualization. **Ignas K. Tonlé:** Writing – review & editing, Supervision, Project administration. **Christine Thobie-Gautier:** Visualization, Validation, Formal analysis. **Estelle Lebègue:** Visualization, Validation, Formal analysis. **Fabiola T. Dontsi:** Writing – original draft, Data curation. **Ranil C.T. Temgoua:** Writing – original draft, Methodology, Investigation, Formal analysis, Data curation, Conceptualization.

Declaration of Competing Interest

The authors declare that they have no known competing financial interests or personal relationships that could have appeared to influence

the work reported in this paper.

Acknowledgements

This work was carried out with financial support from the Centre National de la Recherche Scientifique (CNRS), the Ministère de l'Enseignement Supérieur et de la Recherche in France and the National Agency for Research (project ECLICK ANR- 19-CE07-0021-01 for S.G. and M.B.). RCTT acknowledges the support of the Alexander von Humboldt Foundation through the Humboldt Research Fellowship for Postdoctoral Researchers.

Author Agreement Statement

We the undersigned declare that this manuscript is original, has not been published before and is not currently being considered for publication elsewhere. We confirm that the manuscript has been read and approved by all named authors and that there are no other persons who satisfied the criteria for authorship but are not listed. We further confirm that the order of authors listed in the manuscript has been approved by all of us.

Appendix A. Supporting information

Supplementary data associated with this article can be found in the online version at [doi:10.1016/j.jpba.2024.116147](https://doi.org/10.1016/j.jpba.2024.116147).

References

- [1] C.S.M. Fernandes, G.D.G. Teixeira, O. Irazzo, A.C.A. Roque, Chapter 5 - Engineered Protein Variants for Bioconjugation, in: B. Sarmento, J. das Neves (Eds.), *Biomedical Applications of Functionalized Nanomaterials*, Elsevier, 2018, pp. 105–138, <https://doi.org/10.1016/B978-0-323-50878-0.00005-7>.
- [2] P. Akkapeddi, S.-A. Azizi, A.M. Freedy, P.M.S.D. Cal, P.M.P. Gois, G.J.L. Bernardes, Construction of homogeneous antibody–drug conjugates using site-selective protein chemistry, *Chem. Sci.* 7 (2016) 2954–2963, <https://doi.org/10.1039/C6SC00170J>.
- [3] J. Willwacher, R. Raj, S. Mohammed, B.G. Davis, Selective metal-site-guided arylation of proteins, *J. Am. Chem. Soc.* 138 (2016) 8678–8681, <https://doi.org/10.1021/jacs.6b04043>.
- [4] E.M. Sletten, C.R. Bertozzi, Bioorthogonal chemistry: fishing for selectivity in a sea of functionality, *Angew. Chem. Int. Ed.* 48 (2009) 6974–6998, <https://doi.org/10.1002/anie.200900942>.
- [5] A.P. Taylor, R.P. Robinson, Y.M. Fobian, D.C. Blakemore, L.H. Jones, O. Fadeyi, Modern advances in heterocyclic chemistry in drug discovery, *Org. Biomol. Chem.* 14 (2016) 6611–6637, <https://doi.org/10.1039/C6OB00936K>.
- [6] K. De Bruycker, S. Billiet, H.A. Houck, S. Chattopadhyay, J.M. Winne, F.E. Du Prez, Triazolinediones as highly enabling synthetic tools, *Chem. Rev.* 116 (2016) 3919–3974, <https://pubs.acs.org/doi/full/10.1021/acs.chemrev.5b00599>.
- [7] J. Ohata, M.K. Miller, C.M. Mountain, F. Vohidov, Z.T. Ball, A three-component organometallic tyrosine bioconjugation, *Angew. Chem. Int. Ed.* 57 (2018) 2827–2830, <https://onlinelibrary.wiley.com/doi/full/10.1002/anie.201711868>.
- [8] H. Ban, J. Gavriluk, C.F. Barbas, Tyrosine bioconjugation through aqueous ene-type reactions: a click-like reaction for tyrosine, *J. Am. Chem. Soc.* 132 (2010) 1523–1525, <https://pubs.acs.org/doi/full/10.1021/ja909062q>.
- [9] D. Alvarez-Dorta, C. Thobie-Gautier, M. Croyal, M. Bouzelha, M. Mével, D. Deniaud, M. Boujtita, S.G. Gouin, Electrochemically promoted tyrosine-click chemistry for protein labeling, *J. Am. Chem. Soc.* 140 (2018) 17120–17126, <https://doi.org/10.1021/jacs.8b09372>.
- [10] S. Depienne, M. Bouzelha, E. Courtois, K. Pavageau, P.-A. Lallys, M. Marchand, D. Alvarez-Dorta, S. Nedellec, L. Marín-Fernández, C. Grandjean, M. Boujtita, D. Deniaud, M. Mével, S.G. Gouin, Click-electrochemistry for the rapid labeling of virus, bacteria and cell surfaces, *Nat. Commun.* 14 (2023) 5122, <https://doi.org/10.1038/s41467-023-40534-0>.
- [11] F. Varmaghani, M.T. Ghafari, On the proton-coupled electron transfer of urazole derivatives in pH-unbuffered protic and aprotic solutions: the substituent effect, *J. Electrochem. Soc.* 165 (2018) G155, <https://doi.org/10.1149/2.0071814jes>.
- [12] F. Varmaghani, D. Nematollahi, S. Mallakpour, Oxidative ring cleavage of 4-(4-phenyl)-1,2,4-triazolidine-3,5-diones: electrochemical behavior and kinetic study, *J. Electrochem. Soc.* 159 (2012) F174, <https://doi.org/10.1149/2.111206jes>.
- [13] Y. Shih, J.-M. Zen, A.S. Kumar, P.-Y. Chen, Flow injection analysis of zinc pyriithione in hair care products on a cobalt phthalocyanine modified screen-printed carbon electrode, *Talanta* 62 (2004) 912–917, <https://doi.org/10.1016/j.talanta.2003.10.039>.